Small Changes in Cationic Substituents of Diphenylfuran Derivatives Have Major Effects on the Binding Affinity and the Binding Mode with RNA Helical Duplexes

Min Zhao, Lynda Ratmeyer, Robert G. Peloquin, Shijie Yao, Arvind Kumar, Jaroslaw Spychala, David W. Boykin and W. David Wilson*

Department of Chemistry and Center for Biotechnology and Drug Design, Georgia State University, Atlanta, GA 30303, U.S.A.

Abstract—The interactions of dicationic, 2–4, and tetracationic, 5–7, diphenylfuran analogs of 1 (furamidine) with RNA have been analyzed by thermal melting, spectroscopic, viscometric, kinetic and molecular-modeling techniques. The results of these studies indicate that most of the furan derivatives bind to RNA duplexes by intercalation in contrast to their minor-groove binding mode in AT sequences of DNA, but similar to their binding mode in GC rich regions of DNA. The highest affinity for RNA is found for an imidazoline dication, 2. With some substituents which inhibit formation of a strong intercalation complex, the results suggest a non-intercalative type of binding occurs. The non-intercalative binding probably occurs through a complex with the furan derivative bound in the narrow, deep major groove of A-form RNA helices.

Introduction

A number of clinically useful antimicrobial and anticancer DNA intercalators and groove-binding agents have been discovered.[1] Similarly, some antimicrobial agents that target ribosomal RNA are thought to act by forming a complex with ribosomal RNA.[2] The success of these agents has led to intense efforts to design more efficacious drugs that selectively inhibit functions of nucleic acids in target cells.[3] In the case of DNA binding compounds, the efforts have led to new agents such as the minor-groove binding lexitropsins[4] and covalently linked dimers based on distamycin[5] as well as new intercalators such as the bis-intercalator ditercalinium.[6]

The relatively small amount of high-resolution conformational information and the diversity of conformations for RNA have hindered development of drugs that target RNA. The emergence of pathogenic human RNA viruses such as HIV-1, however, has enhanced the interest in developing new antiviral agents that bind to RNA and inhibit critical functions of the viral genome.[7] The discovery that neomycin is a very strong and selective inhibitor of the binding of the regulatory protein rev to its target RNA, RRE, in the HIV-1 genome[8] clearly demonstrates that drugs that target RNA can be developed as antiviral agents. We have found that an imidazoline analog of the anti-*Pneumocystis carinii* agent, furamidine, 1 (Table 1), binds much more strongly to RNA duplexes than other similar derivatives.[7b] In addition, preliminary testing of furamidine and derivatives in a rev–RRE complex inhibition assay[8] demonstrated a high level of activity (Michael Green, personal communication).

In order to design new derivatives with enhanced RNA interaction selectivity and affinity, it is necessary to understand the RNA complexes of the furan derivatives in more detail, and in particular to determine their RNA binding mode. We report the results of such a study here as well as the synthesis and interaction of new tetracationic furamidine analogs with RNA (Table 1).
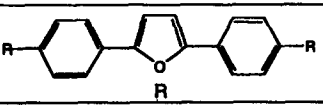
Materials and Methods

Materials

Ethidium bromide was purchased from Sigma. The structure and purity of all compounds were confirmed by ^{1}H NMR and UV-visible spectroscopy. The experiments were conducted in MES buffers (0.01 M 2-(*N*-morpholino)ethane-sulfonic acid, 0.001 M EDTA and pH 6.25) adjusted to 0.1 M (MES10) or 0.2 M (MES20) NaCl concentrations. PolyA·polyU (Sigma) and polydA·polydT (P.L Biochemicals) were characterized as previously described.[9]

Syntheses

Syntheses of 1–4[10] and 8[7d] have been previously published.

2,5-bis-[4-[N-(3-Aminopropyl)amidino]phenyl]furan hydrochloride (5).[10,11] To a suspension of imidate ester hydrochloride (0.65 g, 0.0015 mol) in 10 mL dry ethanol was added 1,3-diaminopropane (0.39 g, 0.0035 mol), and the mixture was stirred at room temperature for 8 h. The reaction mixture became clear, and after a period of time a yellow precipitate appeared. The excess

Table 1. Structures and RNA ΔT_m values

Compound Number		ΔTm^a (°C) of polyA.polyU
1, Furamidine		5.7
2, Furimidazoline		14.4
3		2.5
4		1.3
5		4.0
6		9.1
7		8.5
8		18.1

$^a\Delta T_m$ values are the T_m of the RNA–compound complex - the T_m of the RNA and were determined in MES buffer and 0.1 M NaCl. ΔT_m values for 1–7 with the corresponding DNA polymer are >25 °C while 8 has a ΔT_m value of 6.1 °C.

solvent was removed under vacuum and the solid was treated with ice/water and basified to pH 10 with 1 M NaOH. A gummy mass was separated by decantation, washed with ice/water, dried under vacuum to yield a pale yellow solid.

Recrystallization from ethanol/ether gave 0.45 g (72%) mp 215–216 °C dec. MS m/z 418 (M⁺). The free base 0.41 g (0.001 mol) was suspended in 10 mL ethanolic HCl and stirred for 1 h at 40 °C, the solvent distilled, the residue titrated with dry ether and the hygroscopic yellow solid was filtered and dried under vacuum at 80 °C for 24 h, 0.45 g (85%); mp > 365 °C dec. IR (KBr) 3420, 3130, 2998, 1638, 1607, 1507, 1440, 1375, 1315, 1203, 973, 796, 672 cm⁻¹. ¹H NMR (D₂O/DMSO-d_6) 7.73 (d, 4H, J = 8.2 Hz), 7.52 (d, 4H, J = 8.2 Hz), 6.9 (s, 2H), 3.35 (br, 8H), 1.8 (br, 4H). ¹³C NMR (D₂O/DMSO-d_6) 160.7, 153.8, 135.5, 129.1, 128.3, 125.6, 112.5, 40.3, 19.0. Anal. calcd. for C₂₄H₃₀N₆O·4HCl·H₂O: C, 46.60; H, 6.47; N, 13.59. Found: C, 47.91; H, 6.52; N, 11.63. The low nitrogen analysis may indicate that a significant amount of 5 is hydrolyzed to the amide.

2,5-bis{4-[N-(2-Dimethylaminoethyl)amidino]phenyl}-furan hydrochloride (6).[10,11] Freshly distilled N,N-dimethylethylenediamine (0.46 g, 0.0035 mol) was added to a stirred suspension of imidate ester

hydrochloride (0.065 g, 0.0015 mol) in 25 mL dry ethanol. The mixture was stirred at room temperature for 12 h, the alcohol was distilled under vacuum and the residue was treated with cold water and basified to pH 10 with 1 M NaOH. The yellow precipitate was filtered, washed with water, dried and recrystallized from ethanol 0.52 g (78%); mp 124–125 °C. IR (KBr) 3490, 3285, 1635, 1605, 1375, 1192, 1024, 848, 790, 752, 864 cm⁻¹. ¹H NMR (DMSO-d_6/D₂O) 7.7 (q, 8H), 7.1 (s, 2H), 3.23–3.18 (m, 4H), 3.18–3.13 (m, 4H), 2.13 (s, 12H). ¹³C NMR (DMSO-d_6/D₂O) 157.1, 152.53, 136.0, 127.0, 123.0, 109.1, 59.8, 45.6, 43.5. MS m/z 446 (M⁺).

The free base (0.45 g, 0.001 mol) was dissolved in 10 mL dry ethanol, treated with 10 mL ethanolic HCl, and stirred at 50–60 °C for 2 h. The excess solvent was removed under vacuum and the residue was titrated with dry ether. The solid was filtered, washed with dry ether, dried under vacuum to yield a yellow crystalline solid 0.50 g (90%); mp 280 °C. IR (KBr) 3570, 3400, 3210, 1669, 1610, 1503, 1384, 848, 747 cm⁻¹. ¹H NMR (D₂O/DMSO-d_6/45 °C) 8.0 (d, 4H, J = 7.5 Hz), 7.85 (d, 4H, J = 7.5 Hz), 7.3 (s, 2H), 3.8 (br, 4H), 3.4 (br, 4H), 2.8 (s, 12H). ¹³C NMR (D₂O/DMSO-d_6/45 °C) 164.0, 152.9, 134.6, 129.7, 127.5, 124.4, 112.1, 54.5, 43.4. Anal. calcd for C₂₆H₃₄N₆O·4HCl·1.5H₂O: C, 50.40; H, 6.67; N, 13.56. Found: C, 50.31; H, 6.89; N, 13.48.

2,5-bis-{4-[N-(3-Dimethylaminopropyl)amidino]phenyl}-furan hydrochloride (7).[10,11] Freshly distilled N,N-dimethylaminopropylamine (0.71 g, 0.007 mol) was added to a suspension of imidate ester 1.3 g (0.003 mol) in 20 mL dry ethanol and stirred for 12 h at room temperature. After 2 h the reaction mixture became clear and a solid separated. The solvent was distilled under vacuum and the residue was treated with 20 mL ice/water, basified with 1 M NaOH. The yellow solid was filtered, washed with water, dried and recrystallized from ethanol/ether to yield 1.1 g; mp 131–132 °C, (77%). ¹H NMR (DMSO-d_6/30 °C) 7.83 (s, 8H), 7.16 (s, 2H), 6.41 (br, 4H), 3.14 (t, 4H, J = 6.71 Hz), 2.31 (t, 4H, J = 7.32 Hz), 2.14 (s, 12H), 1.71 (m, 4H, J = 6.71, J = 7.32 Hz). ¹³C NMR (DMSO-d_6/30 °C) 162.1, 152.5, 136.15, 130.5, 126.88, 122.9, 108.9, 57.4, 45.2, 28.0. IR (KBr) 3320, 3134, 2944, 2816, 1669, 1603, 1554, 1377, 1187, 1024, 846, 788, 677 cm⁻¹. MS m/z 474 (M⁺).

The free base 0.95 g (0.002 mol) was suspended in 25 mL dry ethanolic HCl and heated under gentle reflux for 2 h. A bright yellow precipitate formed and the excess solvent was distilled under vacuum. The residue was titrated with 25 mL dry ether and the solid filtered and dried under vacuum at 80 °C (12 h) to give 1.0 g (86%); mp 279–280 °C. IR (KBr) 3310, 3133, 3030, 1615, 1510, 1472, 1285, 1032, 848, 682 cm⁻¹. ¹H NMR (DMSO-d_6) 10.1 (br, 2H), 10.3 (br, 2H), 9.8 (br, 2H), 9.5 (br, 2H), 8.07 (d, 4H, J = 8.8 Hz), 7.97 (d, 4H, J = 8.8 Hz), 7.43 (s, 2H), 3.62–3.57 (m, 4H), 3.23–3.16 (m, 4H), 2.76 (s, 6H), 2.74 (s, 6H), 2.5–2.07 (m, 4H). ¹³C NMR (DMSO-d_6) 162.1, 152.3, 133.8, 129.1, 127.2,

123.6, 111.4, 53.8, 41.9, 22.5. Anal. calcd for $C_{28}H_{38}N_6O\cdot4HCl\cdot1.25H_2O$: C, 52.29; H, 6.97; N, 13.07. Found: C, 52.34; H, 6.98; N, 13.01.

Thermal melting studies

Thermal melting experiments were conducted with a Cary 4 spectrophotometer interfaced to a Dell/486 microcomputer as previously described[12] by following the absorption change at 260 nm as a function of temperature. The temperature was controlled by a Cary temperature controller that was programmed to raise the temperature at a rate of 0.5 °C min^{-1}. A thermistor fixed into a reference cuvette was used to monitor the temperature. Denaturation experiments were conducted with 1.0×10^{-4} M RNA or DNA, and T_m values were determined from first-derivative plots. Compounds are compared by the increase in T_m of the nucleic acid in the presence of the ligand of interest ($\Delta T_m = T_m$ of the complex $- T_m$ of the free nucleic acid) at saturating amounts of the compounds (0.3 mol of compound to nucleic acid base) unless otherwise indicated.

Viscometric titrations

Viscometric titrations were conducted in Ubbelohde semi-micro dilution viscometer (for the Cannon series #75 viscometers) as previously described.[13] One mL of polymer solution (approximately 1×10^{-4} M polyA·polyU phosphate in MES00) was titrated with a stock solution of the desired compound. The additions were made directly into the polyA·polyU solution by using a Hamilton syringe modified to fit into the viscometer mixing chamber.[13]

Absorption and fluorescence

Absorption spectra of the free compounds (Cary 4) were recorded in 1-cm cuvettes in the desired buffer. Small volumes of a solution of concentrated RNA polymer in MES10 and 20 buffer were then titrated into the solution and the absorption spectra rescanned. Fluorescence emission spectra were obtained on an SLM 8000C spectrofluorometer with excitation at 358 nm. Aliquots of DNA or RNA polymer stock solutions were added, and emission spectra collected under the same conditions.

Circular dichroism

CD spectra were obtained with a Jasco J-600 spectrophotometer interfaced to an IBM computer as previously described.[14] All CD experiments were performed at 25 °C in 1-cm path length cuvettes with 4.5×10^{-5} M RNA base concentration. In general spectra were obtained at several ratios of compound to nucleic acid bases in MES10 buffer.

Kinetics

Kinetics measurements were conducted with a Hi-Tech SF-51 stopped-flow spectrometer interfaced to an HP 330 computer as previously described.[15] The SF-51 is equipped with a micromixing chamber and a microcell that allows use of less than 60 μL of sample solution in each mixing event. Single-wavelength kinetic records of absorbance or fluorescence versus time were collected.

Molecular modeling

RNA and DNA duplexes $(rA)_8\cdot(rU)_8$ and $(dA)_8\cdot(dT)_8$ were generated from A- and B-form fiber diffraction data, respectively, by Arnott and co-workers.[16] Both structures were prepared with terminal 5' and 3' OH groups and were energy minimized. The intercalation site geometry in the middle of $(rA)_8\cdot(rU)_8$ was generated based on the crystal structure of an ethidium complex with dinucleotides[17] and by using the methods we have described previously.[18] Distance and torsional constraints were applied to the two central $(rA)_2\cdot(rU)_2$ residues and the hydrogen bonds of all the Watson–Crick A·U base pairs were maintained by distance constraints during energy minimization to create the intercalation site.

The point charges of the compounds were calculated by the MNDO molecular orbital program of the MOPAC module in the SYBYL software package (Tripos). The furan derivatives were then energy refined and manually docked into the intercalation site of $(rA)_8\cdot(rU)_8$ so that each compound had maximum overlap area with the base pairs. Each of the furan derivatives was also manually docked into the minor groove of $(dA)_8\cdot(dT)_8$ and oriented so that there were no significant unfavorable van der Waals interactions. The potential energy equation defined by Kollman and co-workers[19] and a modified version[18a] of the Kollman all-atom force field were used to energy-minimize these complexes. Molecular mechanics calculations were performed using the Tripos SYBYL molecular modeling package on Silicon Graphics Indigo workstations. In all calculations, an RMS gradient of 0.08 kcal mol.Å^{-1} was chosen as the convergence criterion, and a distance-dependent dielectric constant of the form $\varepsilon = 4r_{ij}$ was used.

Results

Binding affinity: thermal melting studies

Affinities of the compounds for the nucleic acids are compared directly by the increases they produce in the T_m of the nucleic acid upon complex formation.[7] The increases in T_m of the RNA polymer, polyA·polyU, and the corresponding DNA polymer, polydA·polydT, are shown in Figure 1 as a function of ratio of compound to nucleic acid for furimidazoline, 2. Both complexes exhibit biphasic melting transitions at low ratios of compound per base pair and monophasic melting behavior at higher ratios. The biphasic transitions are expected at low ratios where separate melting of free and bound nucleic acid regions occurs, while at higher ratios all the nucleic acid binding sites are occupied
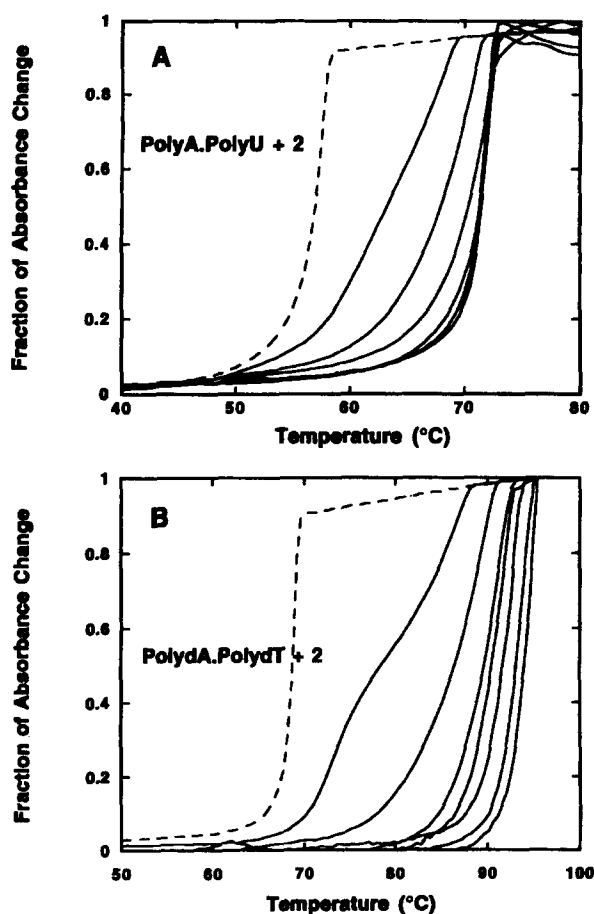
Figure 1. T_m curves in MES10 buffer for (A) polyA·polyU and (B) polydA·polydT [dashed lines] with increasing ratios of 2 [solid lines] from 0.05 to 0.35 mol of compound per nucleic acid base in 0.05 increments, left to right.

and only one transition is observed. The T_m values plateau upon saturation of the binding sites, and our results suggest that saturation occurs at one compound per three to four base pairs in both RNA and DNA.

The increases in the T_m of the RNA polymer at saturation binding, on addition of several furamidine derivatives are compared in Table 1. Furimidazoline 2 gives the largest increase in polyA·polyU T_m in this series. The addition of an extra charged group, as in 5–7, does not increase the ΔT_m of the amidine derivative to the imidazoline ΔT_m value. All of these compounds bind strongly to polydA·polydT and increase its T_m by over 20 °C at saturation as shown for 2 (Fig. 1). Compound 8 is a groove binding agent that has a high T_m for RNA (Table 1), and a lower T_m for DNA (6.1 °C).[7d]

The equilibrium binding constants (K) for interaction of the compounds with DNA and RNA can be calculated from the ΔT_m values at saturation binding.[20a] For a DNA binding site size of three base pairs a K value of approximately 8×10^5 M^{-1} is calculated for a ΔT_m of 20 °C with the $\Delta H°$ value of Breslauer and co-workers[20b] for polydA·polydT. With the $\Delta H°$ value for polyA·polyU from Krakauer and Sturtevant[20c] a Keq of 0.8×10^5 M^{-1} is obtained for a ΔT_m of 5 °C while K is 2.0×10^5 M^{-1}

for a ΔT_m of 10 °C and 4.1×10^5 M^{-1} for a ΔT_m of 15 °C. In all cases the free ligand concentration is approximately 1×10^{-5} M^{-1}.

Analysis of the RNA complexes: spectral changes

In order to obtain additional information on the complexes of the furan compounds with RNA, UV-visible (Fig. 2), fluorescence (Fig. 3) and CD (Fig. 4) spectra were obtained for dication 2 and tetracation 7 with polyA·polyU. Spectra of both 2 (Fig. 2A) and 7 (Fig. 2B) show very pronounced shifts to longer wavelengths and decreases in extinction coefficients on binding to RNA. Spectra for 2 on addition of polydA·polydT are shown in Figure 2C for reference, and it can be seen that both the extinction coefficient decreases and the wavelength shifts are less for the DNA than for the RNA (Fig. 2A) complex.

Fluorescence spectra for complexes with polyA·polyU (Fig. 3A) and polydA·polydT (Fig. 3B) exhibit even larger differences than those found in UV-visible spectra. On addition of RNA, the fluorescence intensity decreases with little shift in the maximum fluorescence wavelength, while the addition of DNA causes the spectrum to shift to lower wavelengths with very little change in intensity. Similar changes were observed with 2 and 7, and results for the complexes with 7 are shown in Figure 3 as examples.
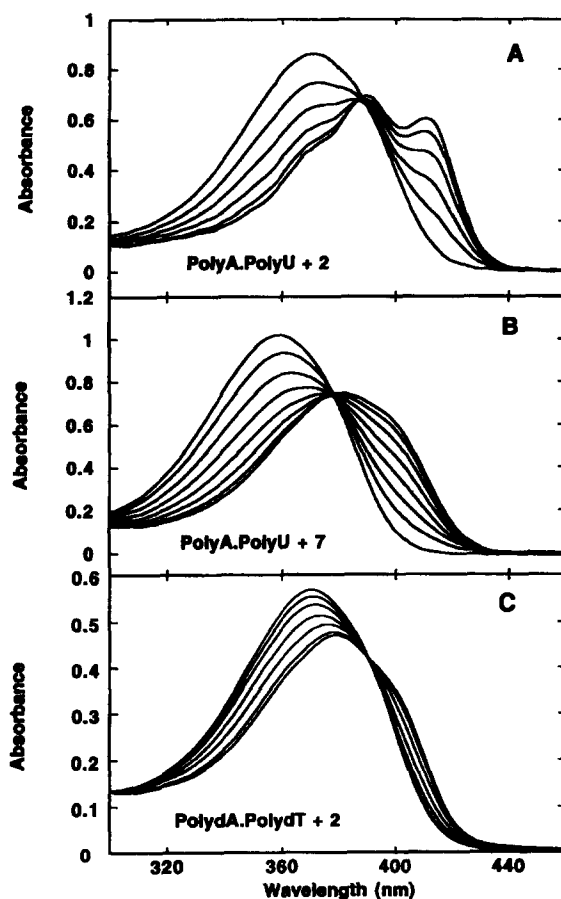

Figure 2. Spectral shifts of 2 on titration with (A) polyA·polyU in MES10 buffer and (C) polydA·polydT in MES20 buffer, and (B) of 7 with polyA·polyU in MES10 buffer. MES20 buffer was used in the DNA experiment because no isosbestic point is observed in MES10.
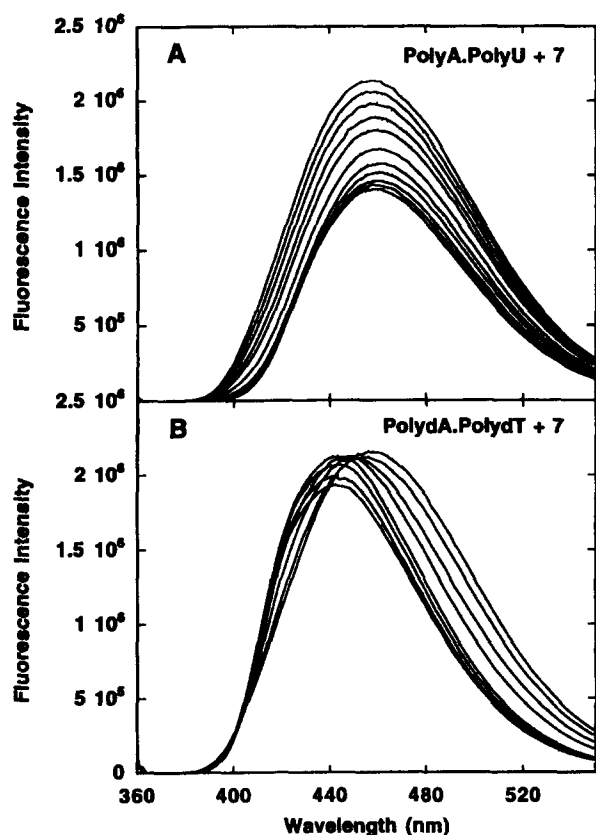
Figure 3. Fluorescence emission spectra in MES10 buffer of **7** with (A) polyA·polyU and (B) polydA·polydT. The excitation wavelength was at 358 nm.

There are pronounced CD spectral changes on complex formation between the furan derivatives and polyA·polyU (Fig. 4). The compounds have no chiral centers and no CD spectra until they complex with the nucleic acid. Significant positive induced CD bands are seen in the 360–400 nm region for **2, 6** and **7** while less intense bands are seen in the same region for **1** and **3**. Smaller negative CD bands are observed in the RNA complexes of these compounds from 300–320 nm. PolyA·polyU has a classical CD spectrum for an A-form RNA helix below 300 nm, and the peak at 260 nm is strongly affected by complex formation with the furans (Fig. 4).

Three different classes of CD behavior are observed with the furan complexes. Compounds **1–3** have positive long wavelength induced CD bands and cause significant *reduction* in the intensity of the 260 nm RNA band. Compounds **4** and **5** have no significant long wavelength induced CD bands, but cause pronounced *increases* in the intensity of the 260 nm RNA band. With **6** and **7**, there are long wavelength induced CD bands as with **1–3**, and these compounds cause an *increase* in intensity of the RNA 260 nm band as with **4** and **5**. The increases at 260 nm for **6** and **7** are smaller than those observed for complexes with **4** and **5**. The RNA groove-binding agent[7d] **8** causes slight increases in the intensity of the 260 nm RNA CD band. There are no long wavelength absorption transitions for **8**.

Compounds **1–3** cause only small changes in the RNA CD bands below 260 nm while the intensities of these bands are significantly increased on complex formation with **4–7**. These results clearly demonstrate that the complexes formed with the furan derivatives have very significant variations in their RNA complexes as the nature of the cationic group is changed.

RNA binding mode

Classical intercalation causes an increase in the length of nucleic acids and an increase in their solution viscosity.[1] The changes in viscosity of polyA·polyU solutions on titration with several furans as well as the classical intercalator ethidium bromide are compared in Figure 5. As expected, ethidium bromide causes large increases in the viscosity of the RNA polymer solutions that reaches a plateau at saturation of binding sites on the RNA. Furans **1** and **7** cause increases in viscosity of polyA·polyU solutions which are approximately one half the increase induced by ethidium bromide in the plateau region while furimidazoline causes increases similar to those observed with ethidium bromide. Tetracation **5** causes initial small increases in viscosity that are followed by decreases as site saturation is approached. Addition of other cations, such as **8**, which cause large increases in the RNA T_m, do not cause significant increases in the RNA viscosity.

For compounds with the same charge the variation of the dissociation rate constant (k_d) with salt concentration for nucleic acid complexes is also sensitive to the binding mechanism and, thus, to the binding mode.[16,21] Log k_d is plotted versus log $[Na^+]$ in Figure 6 for dicationic furans **1–3** as examples. The slopes for all plots are -0.7 ± 0.07 for the RNA complexes in agreement with an intercalative binding mode.[16,21] Similar plots for complexes with DNA all have slopes near -1.7 in agreement with a groove-binding interaction.[16,21] The magnitudes of the k_d values in the different salt concentrations are in agreement with the ΔT_m values from Table 1. Furimidazoline has the highest ΔT_m and the lowest dissociation rate constant. The RNA complexes with furamidine and **3** have significantly lower ΔT_m values (Table 1), and the compounds dissociate from RNA complexes 50–100 times faster than furimidazoline.

Molecular modeling

In order to obtain additional information about the molecular basis for the favorable interactions of furimidazoline with RNA we have conducted comparative molecular modeling experiments on the RNA complexes of the dications **1–4**. The four compounds were docked into an intercalation site, constructed as described in the methods section, in the center of the sequence $A_8 \cdot U_8$ as a model for polyA·polyU, and the complexes were then energy minimized. Views of the complex of **2** with the RNA intercalation site are shown in Figure 7 as examples for
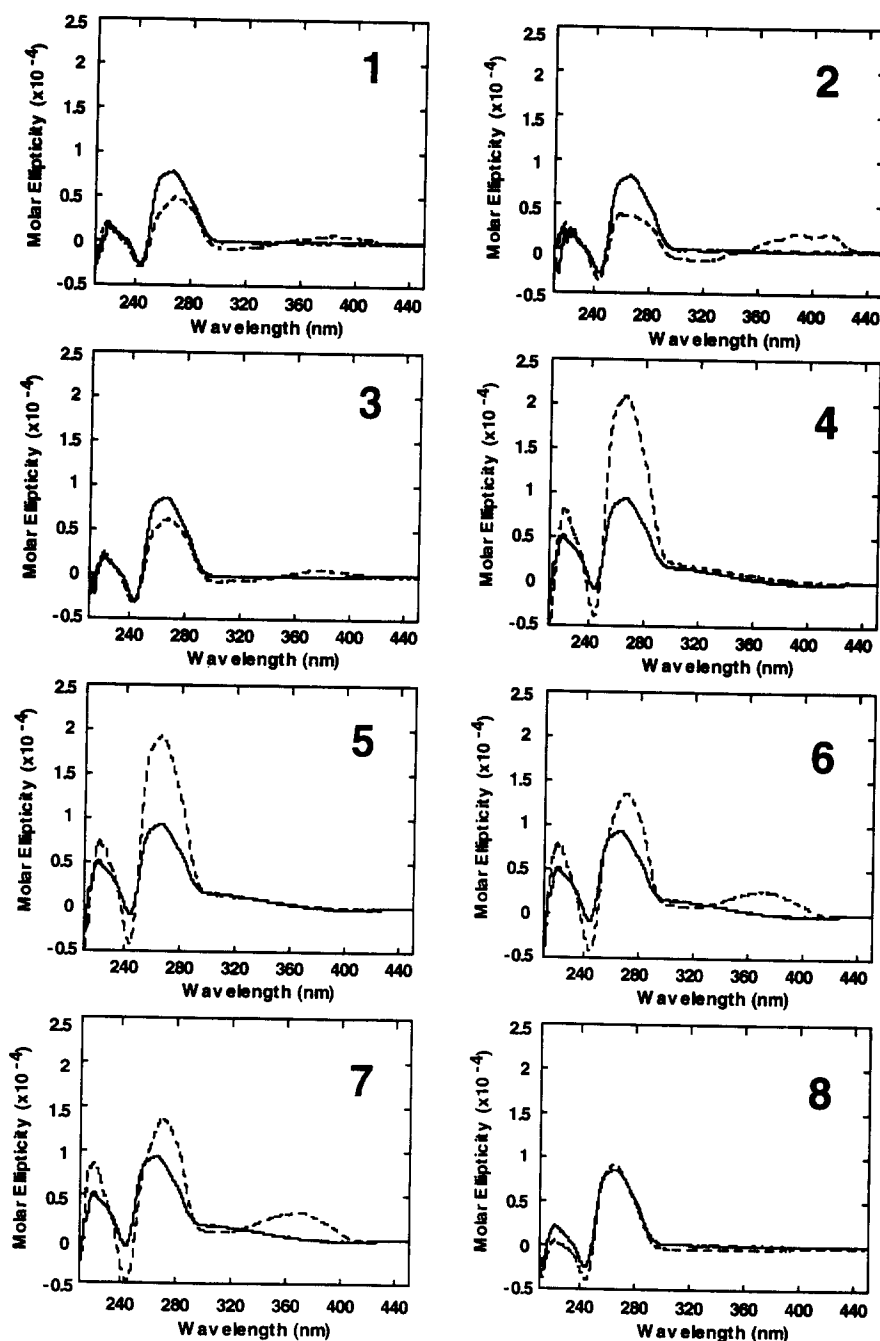
Figure 4. CD spectra for polyA·polyU (4.5 × 10⁻⁵ M nucleic acid base concentration, solid lines) in MES10 buffer with compounds 1–8 (dashed lines) at a ratio of 0.3 mol of compound per mol of nucleic acid base.

furan intercalation. The imidazoline ring of **2** is in the diphenylfuran plane while the amidine of **1** and the tetrahydropyrimidine cationic group of **3** are twisted by approximately 30° out of the plane due to van der Waals repulsion. The imidazoline N–H groups that point into the helix form hydrogen bonds with the anionic oxygens on the phosphate groups at the intercalation site (N to O distance of 2.8 Å). The larger twist in **1** and **3** causes the intercalating system of these compounds to be shifted slightly out of the intercalation site, relative to the imidazoline complex, towards the major groove, and this weakens the interactions with RNA.

The binding energies are calculated by subtracting the energies of the minimized RNA and minimized furan compound from the energy of the minimized complex. The calculated binding energy values rank in the same order as observed for the compounds in the T_m studies (Table 1): **2**, -21.6 kcal mol^{-1} < **1**, -17.8 kcal mol^{-1} < **3**, -16.7 kcal mol^{-1} < **4**, -14.3 kcal mol^{-1}. Although the absolute values of the calculated energies cannot be compared directly to experimental energies, the relative values agree with the experimental results, and the minimized geometries can give considerable insight into the reasons for the variation in affinities of these compounds with RNA. Docking of the furans with
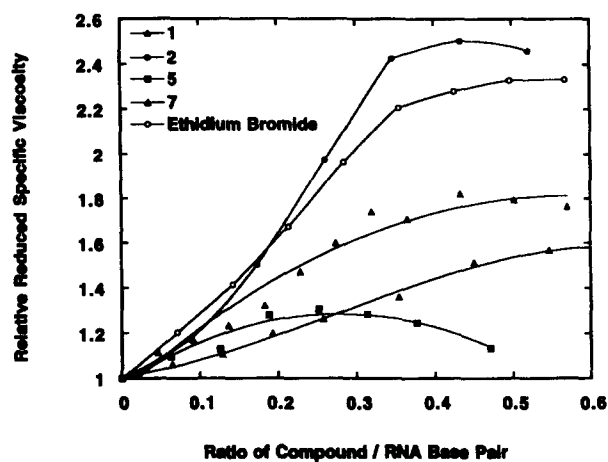
Figure 5. Viscometric titrations of polyA·polyU with ethidium bromide (O), 1 (▲), 2 (●), 5 (■), and 7 (△) in MES10 buffer.
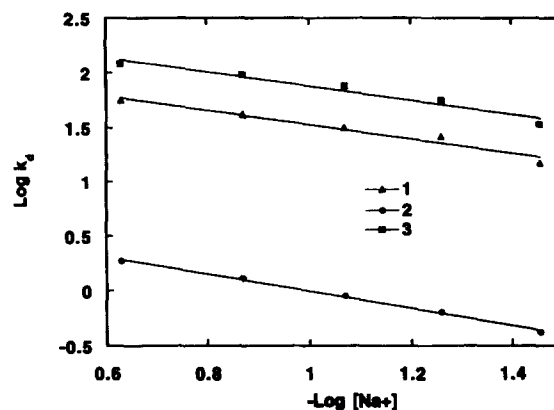
Figure 6. Plots of log k_d vs −log[Na⁺] for dissociation of compounds 1 (▲), 2 (●) and 3 (■) from polyA·polyU in MES buffer with NaCl added to give the desired [Na⁺].
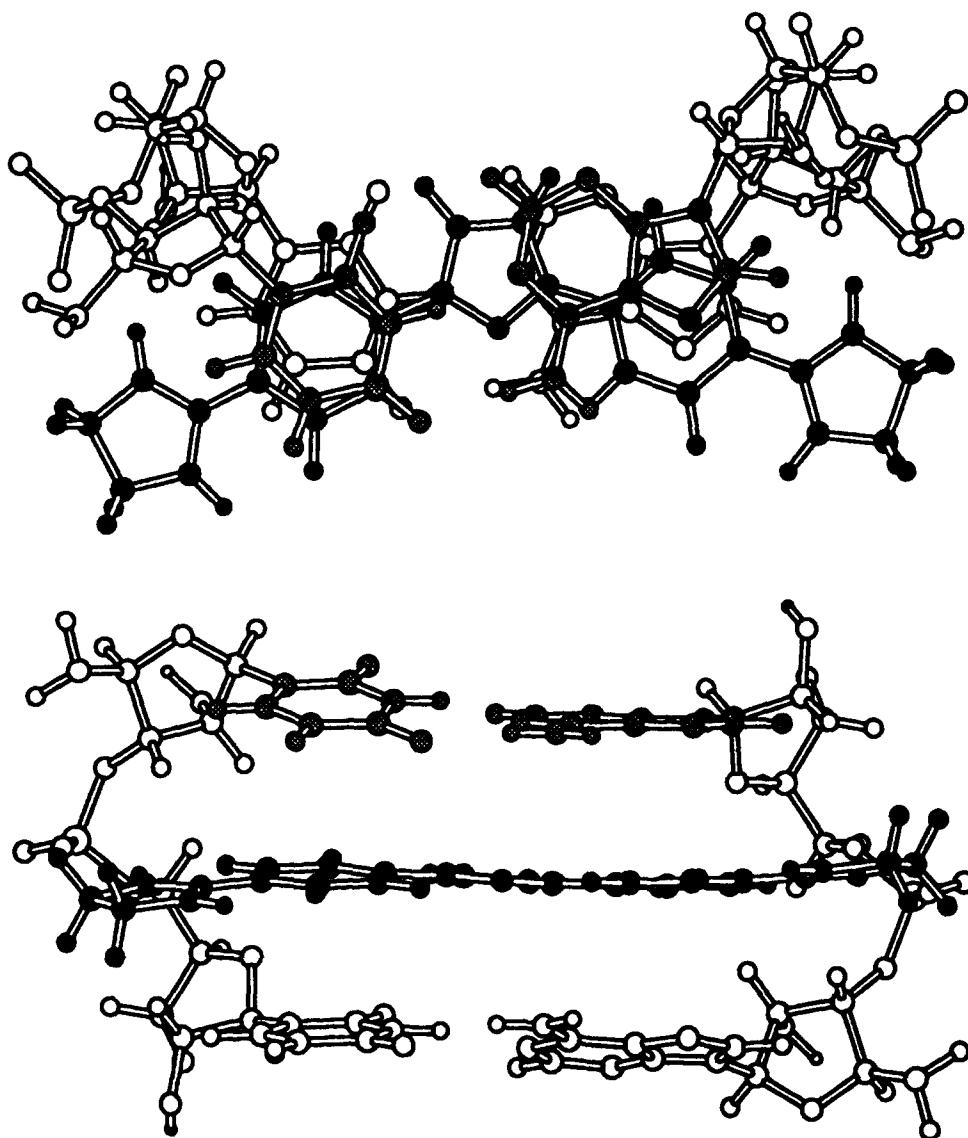

Figure 7. Views of an energy-minimized complex of furimidazoline intercalated into A₈U₈. Only the base pairs on each side of the compound are shown for clarity. The atoms in the base pair above the intercalated compound are in gray while the atoms in the base pair below are white, and the atoms in the compound are black. The top view is looking down the RNA duplex helix axis with the minor groove at the top and the major groove below the view shown. The imidazoline substituents can be seen at the edges of the major groove and each of the two N–H groups that point into the RNA backbone region forms a hydrogen bond with an anionic phosphate oxygen. The lower view in the Figure is looking into the intercalation site from the major groove, and shows that the unfused aromatic system is able to assume an essentially planar conformation that is very close to the energy minimum for the unbound compound.

intercalation sites based on X-ray crystallographic results from complexes with other intercalators causes changes in the absolute values of the energies, but the scaling and relative values remain similar to the results obtained for the ethidium bromide site. The conclusions from the modeling studies are, thus, general.

Modeling of the interactions of the dicationic furan derivatives with the minor groove of a $dA_8 \cdot dT_8$ DNA sequence gave a significantly more negative (favorable) binding energy for the compounds with the DNA groove than with the RNA intercalation site in agreement with the observed larger ΔT_m values for DNA than for RNA complexes (Fig. 1, Table 1).

Discussion

As shown in Table 1, furimidazoline binds significantly better to RNA than the other dications, 1, 3 and 4. Addition of charged amines to furamidine, as in 5–7, does not raise the ΔT_m to the imidazoline value, under these conditions. The imidazoline tetracation 8, which is an RNA groove-binding agent,[7d] and the intercalator ethidium bromide[7a] both have high RNA ΔT_m values, and these results indicate that the magnitude of the RNA T_m increases on complex formation cannot give specific information on the compound binding mode. It is now well established that the furan derivatives bind to AT sequences in DNA in the minor groove,[10] but there is considerable evidence that they bind to GC sequences in DNA, where minor-groove binding is less favorable, by intercalation.[21a] Although there is considerable information about complexes of small organic cations with DNA, much less is known about similar complexes with RNA, and we have conducted a systematic set of studies to determine the molecular basis for the favorable binding of 2 to RNA. This type of information on RNA complexes is essential for our experiments to design structure-specific RNA antiviral drugs.[7] In addition, RNA interactions can be a source of significant drug loss for drugs designed to target DNA, and it is essential to establish ways to prevent RNA binding when it is not desired. Compound 4, for example, actually binds to DNA slightly more strongly than furimidazoline, but it binds to RNA much more weakly.

Spectral shifts in the region between 300–500 nm, where RNA does not absorb, reveal extinction coefficient decreases and large shifts to longer wavelengths for all of the furans on complex formation with RNA (Fig. 2). These spectral changes are much larger than observed for the minor-groove AT DNA complexes of the furan compounds (Fig. 2C), even though the compounds bind more strongly to the AT regions of DNA (Table 1). We have previously found spectral shifts similar to those observed with RNA when unfused aromatic cations bind to GC sequences in DNA, and we found that for such compounds the shifts correlated with an intercalation binding mode.[21a,22]

The fluorescence changes induced in the furan on complex formation with RNA are also large, and represent a decrease in intensity (Fig. 3). With the DNA minor-groove complex the changes are quite different and there is little decrease in fluorescence intensity (Fig. 3). These changes again suggest a significantly different binding mode for the furan derivatives with RNA and with AT sites in DNA. The fluorescence changes observed for the RNA–furimidazoline complexes are similar to those observed previously on formation of intercalation complexes with GC sites in DNA.[21a]

The CD spectral changes induced on complex formation provide very useful comparative information. The induced CD bands for the furan derivatives 1–3, 6 and 7 are positive in the region above 350 nm where there is a strong absorption band for the furan and no interference from RNA CD bands. The induced bands for the imidazoline derivative in this region are stronger than for the other dicationic furans 1 and 3 suggesting an optimum stacking interaction for furimidazoline with the RNA base pairs (Fig. 4). The dicationic furans 1–3 cause a significant decrease in the large positive RNA CD band near 260 nm (Fig. 4) while the RNA groove-binding agent 8 causes a small increase in the same band. These CD changes suggest that the furans cause a significant conformational change in RNA on complex formation, in agreement with an intercalation model, while 8 causes no large change in RNA conformation, in agreement with a groove interaction for 8. The binding model for 1–3 suggested by all of the spectral comparisons involves stacking of the diphenylfuran aromatic system with RNA base pairs in an intercalation complex. The intense induced CD bands for the furimidazoline indicates that its aromatic system interacts strongly with the base pairs at the intercalation site. The reduced intensity of the induced CD bands observed with 1, 3 and 4 indicate that they are not as centrally located with respect to the base pairs in the intercalation site[23] in good agreement with the molecular modeling results.

A kinetic method for distinguishing intercalation from groove interactions is based on the different mechanisms for formation of the two types of complexes and is particularly useful in establishing sequence-specific binding modes.[21,22] Groove complexes form at close to a diffusion-controlled rate while intercalation complexes form through an initial externally bound complex that intercalates when it encounters a thermally opened base-pair site that is appropriate for intercalation. Evaluation of the salt concentration dependence of the association and/or dissociation rate constants is one method for distinguishing between these two mechanisms.[21,22] For dications the slope of a log k_d versus –log [Na$^+$] plot is predicted to be approximately –0.7 for intercalation while the slope for a dicationic groove-binding agent is predicted to be –1.7. The slopes in Figure 6 are all –0.7 ± 0.1, again in agreement with an intercalation binding mode for furan derivatives 1–3 with RNA. In addition,

the dissociation rate constant for furimidazoline (see Fig. 6) is much lower than for 1 and 3. Since intercalators which are similar in structure and have the same charge tend to have very similar association rate constants, the lower k_d value for furimidazoline is in agreement with significantly stronger binding of that compound to RNA. A very important additional conclusion from these kinetic studies is that the cationic groups of the furans are located in the same groove. If the bulky cationic groups of furans such as 3 were located in opposite grooves (threading intercalation), then their binding kinetics, both association and dissociation, would be significantly slower than for furans with smaller substituents, such as 1, and this is clearly not the observed result (see Fig. 6).

The intercalation binding model for furimidazoline is strongly supported by the large increases in viscosity induced on complex formation with RNA (Fig. 5). Solution viscosity increases are one of the classical methods used to establish an intercalation binding mode for nucleic acid complexes, and the method is among the most reliable techniques for distinguishing between intercalation and groove-binding modes.[1] The viscosity increases observed for furamidine 1 and for tetracation 7 are less than for furimidazoline 2 and could indicate some distortion in their intercalation complexes or some combination of intercalation and groove-binding modes. The small viscosity increases observed for RNA–5 complexes may indicate that a significant amount of the compound has been hydrolyzed to an amide.

All of the experimental results suggest binding modes that are significantly different for 4 relative to 1–3. Compound 4 is a dication of similar structure to 1–3 but it causes only a small increase in T_m of polyA-polyU, and it does not have significant long wavelength induced CD bands. In contrast to the reduction in intensity of the 260 nm CD band observed on complex formation of 1–3 with RNA, the band increases in intensity in the presence of 4. A similar increase, with no long wavelength induced CD bands is observed for 5. The CD results for 4 are similar to those for 8, although they cause larger changes in the RNA band than 8, and we feel that the binding mode that best explains the interaction of 4 with RNA is groove binding. The switch from intercalation to groove binding with this compound is probably a combined result of decreased intercalation affinity and enhanced groove binding. The intercalation affinity is optimal for the imidazoline substituent and decreases for the other cationic groups. The larger hydrophobic groups of 4 are especially difficult to incorporate into an intercalation complex, but may have favorable contacts in an RNA groove complex.

Compound 5 behaves more like a polyamine such as 8, with amino groups that can interact strongly with the closely spaced phosphate groups in the RNA major groove in a groove complex. Apparently, the dimethylamino groups of 6 and 7 favor an intercalation binding mode and they provide some additional

favorable interactions in the intercalation complex. Both 6 and 7 have the long wavelength induced CD bands observed with RNA complexes of 1–3, but they cause increases in the RNA 260 nm CD band that are smaller but similar to the effects observed with 4. As observed with 4, but not with 1–3, 6 and 7 cause significant increases in the intensities of the RNA CD bands at wavelengths below 260 nm. The model for the RNA complexes of 6 and 7 suggested by all of these observations involves intercalation of the diphenylfuran aromatic system, as with 1–3, with the terminal cationic amines of 6 and 7 interacting with phosphate groups in the major groove as with 8. The CD spectra for 6 and 7 are, thus, a combination of those observed for 1–3 and for 4. We are synthesizing additional compounds to test these proposed binding models for the tetracationic furan derivatives.

The observations from the experiments described above provide the initial information for molecular modeling of the dicationic furan derivatives with RNA: an intercalation binding mode with both cationic substituents in the same major groove in the complex. The two cationic groups of these compounds were placed in the major groove, since unacceptable steric clash was found with the substituents in the minor groove, and the diphenylfuran aromatic system was stacked into the intercalation site. Analysis of the models of dications 1–4 with the intercalation site reveals some clear reasons for the strong binding of furimidazoline to RNA. The N–C–N bond angle in the five membered imidazoline ring is smaller than in the other three compounds and this leads to a smaller torsional angle between the imidazoline ring and the phenyl group than is observed with the other compounds. The planar imidazoline groups are able to slide more deeply into the intercalation site than the smaller amidine groups which have 30–35° twist with respect to the phenyl ring (the phenyl–imidazoline twist is approximately 0°). As the cationic group is enlarged to six (3) and seven-membered (4) rings, the twist with respect to the phenyl ring is again approximately 30° and the out of plane groups of the larger cation rings cause additional steric clash with the bases at the intercalation site for the optimum stacking geometry with the diphenylfuran aromatic system.

As can be seen from Figure 7, the -NH groups of the imidazoline that point towards the RNA backbone are close to the phosphate at the intercalation site, and form a strong hydrogen bond with an anionic phosphate oxygen. For 1 and 3 to form such a hydrogen bond, their torsional angles must be reduced at a significant cost in energy. The modeling energies and experimental ΔT_m values, thus, both predict the order of stability of the furan–RNA complexes to be: furimidazoline > furamidine > 3 > 4. The molecular basis for the differences in RNA affinity for these dications involves fit into the intercalation site and stacking of the diphenylfuran system with the base pairs at the intercalation site. As discussed above, the intercalation affinity of 4 is reduced to such a degree that it

apparently switches to a weak RNA groove-binding mode.

References

1. (a) Waring, M. J. *The Molecular Basis of Antibiotic Action*, p. 287, 2nd Edn, Gale, E. F.; Cundliffe, E.; Reynolds, P. E.; Richmond, M. H.; Waring, M. J., Eds; Wiley; New York, 1981; (b) Wilson, W. D. *Nucleic Acids in Chemistry and Biology*, Chapter 8, Blackburn, M.; Gait, M., Eds; IRL Press Ltd; Oxford, 1990; (c) *Advances in DNA Sequence Specific Agents*, Hurley, L. H., Ed.; JAI Press Inc.; Greenwich, CT, 1992; (d) Tidwell, R. R.; Jones, S. K.; Naimen, N. A.; Berger, L. C.; Brake, W. B.; Dykstra, C. C.; Hall, J. E. *Antimicrob. Agents Chemo.* 1993, *37*, 1713.

2. Cundliffe, E. *The Ribosome: Structure, Function, and Evolution*, pp. 479–490, Hill, W. E.; Dahlberg, A.; Garrett, R. A.; Moore, P. B.; Schlessinger, D.; Warner, J. R., Eds; American Society for Microbiology; Washington, D.C., 1990 and references therein.

3. (a) Haseltine, W. A. *J. AIDS* 1989, *2*, 311; (b) Broder, S. *Concepts in Viral Pathogenesis III*, pp. 337–351, Notkins, A.; Oldstone, M., Eds; Springer-Verlag; Berlin, 1989; (c) Mitsuya, H.; Yarchoan, R.; Broder. S. *Science* 1990, *249*, 1533. (d) *Design of Anti-AIDS Drugs*, Vol. 14, DeClercq, E., Ed.; Elsevier, Pharmacochemistry Library Series, 1990.

4. Lown, J. W. *Jerusalem Symposia on Quantum Chemistry and Biochemistry*, Vol. 23, Pullman, B.; Jortner, J., Eds; Kluwer Academic Publishers, 1990.

5. (a) Geierstanger, B. H.; Jacobsen, J. P.; Mrksich, M.; Dervan, P. B.; Wemmer, D. E. *Biochemistry* 1994, *33*, 3055; (b) Mrksich, M.; Dervan, P. B. *Science* 1991, *116*, 3663; (c) Geierstanger, B. H.; Mrksich, M.; Dervan, P. B.; Wemmer, D. E. *Science* 1994, *266*, 646.

6. (a) Peek, M. E.; Lipscomb, L. A.; Bertrand, J. A.; Gao, Q.; Roques, B. P.; Jaureguiberry, C.; Williams, L. D. *Biochemistry* 1994, *33*, 3494; (b) Lambert, B.; Segal-Bendirdjian, E.; Roques, B. P.; LePecq, J.-B. *DNA Repair Mechanisms and Their Biological Implications in Mammalian Cells*, pp, 639–652, Lambert, M. W.; Laval, J., Eds; Plenum Press; New York, 1988.

7. (a) Ratmeyer, L. S.; Vinayak, R.; Zon, G.; Wilson, W. D. *J. Med. Chem.* 1992, *35*, 966; (b) Wilson, W. D.; Ratmeyer, L.; Zhao, M.; Strekowski, L.; Boykin, D. *Biochemistry* 1993, *32*, 4098; (c) Wilson, W. D.; Ratmeyer, L.; Cegla, M. T.; Spychala, J.; Boykin, D.; Demeunyck, M.; Lhomme, J.; Krishnan, G.; Kennedy, D.; Vinayak, R.; Zon, G. *New J. Chem.*

1994, *18*, 419; (d) McConnaughie, A. W.; Spychala, J.; Zhao, M.; Boykin, D.; Wilson, W. D. *J. Med. Chem.* 1994, *37*, 1063.

8. Zapp, M. L.; Stern, S.; Green, M. R. *Cell* 1993, *74*, 969.

9. Tanious, F. A.; Veal, J. M.; Buczak, H.; Ratmeyer, L. S.; Wilson, W. D. *Biochemistry* 1992, *31*, 3103.

10. Boykin, D. W.; Kumar, A.; Spychala, J.; Zhou, J.; Lombardy, R. J.; Wilson, W. D.; Dykstra, C. C.; Jones, S. K.; Hall, J. E., Tidwell, R. R.; Laughton, C.; Nunn, C. M.; Neidle, S. *J. Med. Chem.* 1995, *38*, 912.

11. Spychala, J.; Boykin, D. W.; Wilson, W. D.; Zhao, M.; Tidwell, R. R.; Dykstra, C. C.; Hall, J. E.; Jones, S. K; Schinazi, R. F. *Eur. J. Med. Chem.* 1994, *29*, 363.

12. Kibler-Herzog, L.; Kell, B.; Zon, G.; Shinozuke, K.; Mizan, S.; Wilson, W. D. *Nucleic Acids Res.* 1990, *18*, 3545.

13. Jones, R. L.; Davidson, M. W.; Wilson, W. D. *Biochim. Biophys. Acta* 1979, *561*, 77.

14. Zuo, E. T.; Tanious, F. A.; Wilson, W. D.; Zon, G.; Tan, G.-S.; Wartell, R. M. *Biochemistry* 1990, *29*, 4446.

15. (a) Wilson, W. D.; Tanious, F. A.; Barton, H. J.; Jones, R. L.; Fox, K.; Wydra, R. L.; Strekowski, L. *Biochemistry* 1990, *29*, 8452; (b) Tanious, F. A.; Yen, S.-F.; Wilson, W. D. *Biochemistry* 1991, *30*, 1813.

16. (a) Arnott, S.; Hukins, D. W. L.; Dover, S. D. *Biochem. Biophys. Res. Commun.* 1972, *48*, 1392; (b) Chandrasekaran, R.; Arnott, S. *Landolt-Bornstein, Nucleic Acids, VII/1b*, p. 55, Saenger, W., Ed.; Springer-Verlag; Berlin, 1989.

17. Jain, S. C.; Sobell, H. M. *J. Biomol. Struc. Dyn.* 1984, *1*, 1179.

18. (a) Veal, J. M.; Wilson, W. D. *J. Biomol. Struc. Dyn.* 1991, *8*, 1119; (b) Yao, S.; Wilson, W. D. *J. Biomol. Struc. Dyn.* 1992, *10*, 367.

19. Weiner, S. J.; Kollman, P. A.; Nguyen, D. T.; Case, D. A. *J. Comp. Chem.* 1986, *7*, 230.

20. (a) Crothers, D. M. *Biopolymers* 1971, *10*, 2147; (b) Marky, L. A.; Curry, J.; Breslauer, K. J. *Molecular Basis of Cancer*, p. 155, Alan R. Liss Inc.; New York, 1985; (c) Krakauer, H.; Sturtevant, J. M. *Biopolymers* 1968, *6*, 491.

21. (a) Wilson, W. D.; Tanious, F. A.; Buczak, H.; Venkatramanan, M. K.; Das, B. P.; Boykin, D. W. *Molecular Basis of Specificity in Nucleic Acid–Drug Interactions*, pp. 331–353, Pullman, B.; Jortner, J., Eds; Kluwer Academic Publishers; The Netherlands, 1990; (b) Wilson, W. D.; Tanious, F. A. *Molecular Aspects of Anticancer Drug–DNA Interactions*, Vol. 2, pp. 243–269, Neidle, S.; Waring, M. J., Eds; The Macmillan Press; London, 1994.

22. Tanious, F. A.; Spychala, J.; Kumar, A.; Greene, K.; Boykin, D. W.; Wilson, W. D. *J. Biomol. Struc. Dyn.* 1994, *11*, 1063.

23. (a) Norden, B.; Tjerneld, F. *Biopolymers* 1982, *21*, 1713; (b) Lyng, R.; Hard, R.; Norden, B. *Biopolymers* 1987, *26*, 1327.